

Surface-Plasmon-Polariton Assisted Diffraction in Periodic Subwavelength Holes of Metal Films with Reduced Interplane Coupling

Xu Fang, Zhiyuan Li, Yongbing Long, Hongxiang Wei, Rongjuan Liu, Jiyun Ma, M. Kamran, Huaying Zhao, Xiufeng Han, Bairu Zhao, and Xianggang Qiu*

Institute of Physics and Beijing National Laboratory for Condensed Matter Physics, Chinese Academy of Sciences, Beijing 100080, China

(Received 18 December 2006; published 10 August 2007)

Metal films grown on an Si wafer perforated with a periodic array of subwavelength holes have been fabricated and anomalous enhanced transmission in the midinfrared regime has been observed. High order transmission peaks up to Si(2, 2) are clearly revealed due to the large dielectric constant contrast of the dielectrics at the opposite interfaces. The Si(1, 1) peak splits at oblique incidence both in TE and TM polarization, which confirms that anomalous enhanced transmission is a surface-plasmon-polariton (SPP) assisted diffraction phenomenon. Theoretical transmission spectra agree excellently with the experimental results and confirm the role of SPP diffraction by the lattice.

DOI: [10.1103/PhysRevLett.99.066805](https://doi.org/10.1103/PhysRevLett.99.066805)

PACS numbers: 73.20.Mf, 42.25.Bs, 42.70.Qs, 78.67.-n

Since the discovery of anomalous enhanced transmission of subwavelength metallic hole arrays in 1998 [1], enormous interest has been sparked worldwide among researchers due to its potential application in subwavelength optoelectronic devices as well as the underlying physics. Although the exact origin of the enhanced transmission remains controversial [2,3], it is generally acknowledged that surface plasmon polaritons (SPPs) play a crucial role. Recent research indicates that this phenomenon could be a SPP assisted diffraction process [4,5]. In this process, the coupling of SPPs on the opposite interfaces of the metal film helps the electromagnetic energy to tunnel through the subwavelength holes [6]. This interplane coupling is substantial when the dielectrics at the interfaces are similar, and is the strongest when they are identical [7]. To achieve high transmittance, most previous work adopts either free standing films or films on substrates with small dielectric constants. However, the strong interplane interference in these kinds of samples will hinder the mechanism from getting fully revealed [8]. For thin films with identical interfaces, this interference could even lift the degeneracy of SPPs on the two interfaces and alter their modes [9,10]. So it is of great interest to reduce the interference in order to study the underlying physics of the SPPs at each individual interface. For this purpose, we adopt the air/Au/Si system in which air and Si have a large difference in their dielectric constants in the midinfrared regime. The thickness of the metal films is an order larger than the skin depth (about 20 nm for Au at the midinfrared regime). It is expected that in such systems the interference of the SPP modes at two interfaces is greatly reduced and the characteristics of SPPs at a single interface are preserved.

Metal films were deposited on an Si wafer by magnetic sputtering. The hole arrays were fabricated by conventional ultraviolet photolithography and reactive ion etch-

ing. All the patterns are square arrays of circular holes, occupying an area of $7 \times 7 \text{ mm}^2$, respectively. The hole number for each pattern is over 1×10^6 and the finite size effect is assumed to be well avoided [11]. The infrared transmittance spectra were obtained with an ABB Bomem DA8 Fourier transform infrared spectrometer.

Shown in Fig. 1(a) is the zeroth-order transmittivity (transmittance normalized by the porosity of the film) of three Au films under normal incidence. All three films have a thickness of 320 nm and a hole diameter of $3 \mu\text{m}$. The lattice constants are $5 \mu\text{m}$ (sample A), $6 \mu\text{m}$ (sample B), and $7 \mu\text{m}$ (sample C), respectively. The transmission peaks can be assigned with various orders according to Eq. (1) as follows. Three salient features can clearly be discerned. (i) Because the dielectric constant of Si ($\epsilon = 11.7$) is much larger than that of air in the midinfrared regime, the distance between air(1, 0) and Si(1, 0) is greatly expanded in comparison with previous reports [Si(1, 0) are at 21.02 and 24.41 μm for samples B and C, respectively, which are not shown in the figure]. (ii) High order peaks such as Si(1, 1), (2, 0), and (2, 1) can be clearly observed between air(1, 0) and Si(1, 0). (iii) Peaks with the same order of the three samples shift according to the periodicities, and they have larger wavelengths for larger periodicities. Numerical calculations on the transmission spectra have been performed by means of a transfer-matrix method combined with an analytical modal solution [12], using the same material parameters as in the experiments, and the results are displayed in Fig. 1(b). The circular holes are treated as square ones with the same area, considering the convenience in modeling. A series of resonant peaks can be clearly found and their positions agree well with the experimental data.

We attribute the above observation to be a result of SPP assisted diffraction process. SPPs have different momenta from light of the same energy [13]. The gap between the

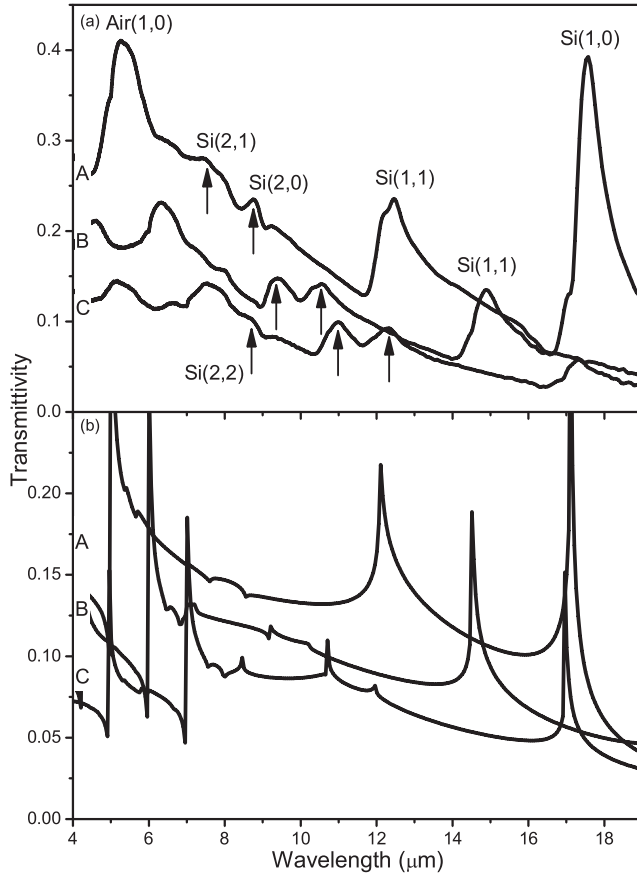


FIG. 1. (a) Experimental and (b) theoretical results of transmittivity of subwavelength hole arrays on Au films. Air stands for the air/Au interface and Si stands for the Si/Au interface. The periodicities are $5 \mu\text{m}$ (sample A), $6 \mu\text{m}$ (sample B), and $7 \mu\text{m}$ (sample C), respectively.

momenta can be compensated with the presence of a periodic hole array. The momentum matching condition is

$$\vec{k}_{\text{sp}} = \vec{k}_{\parallel} \pm i\vec{G}_x \pm j\vec{G}_y, \quad (1)$$

where k_{sp} is the wave vector of SPPs, k_{\parallel} is the in-plane wave vector component of the incident light (zero for normal incidence), i and j are integers, G_x and G_y are the reciprocal vectors [14]. These two indices have been used to designate the resonant peaks in Fig. 1(a). We have extracted the experimental SPPs dispersion from the data shown in Fig. 1(a) through Eq. (1) and compared with the theoretical one which adopts the material parameters in Refs. [15,16], and found that these two curves fit very well.

To further confirm the above findings, we measured the angular dependent transmittivity of sample D (thickness 220 nm , periodicity $5 \mu\text{m}$, and hole diameter $3 \mu\text{m}$). The incident angle varies from 0° to 36° , with a 4° increment. Under TM polarization (polarization perpendicular to the rotation pole), Si(1,0) and Si(1,1) split into two branches. The data for Si(1,1) are shown in Fig. 3. Under TE polar-

ization (polarization parallel to the rotation pole), Si(1,0) undergoes minor blueshift (from $17.63 \mu\text{m}$ at 0° to $17.46 \mu\text{m}$ at 36°) while Si(1,1) splits with the splitting getting larger with the increasing angle, as shown in Fig. 2(a). This is the only report that shows peak splitting under TE polarization up to now. The theoretical spectra, as displayed in Fig. 2(b), reproduce the experimental data excellently.

SPPs have p -wave-like character and the electric field lies parallel with their propagation direction. They can be excited if the incident light has a component of the electric field parallel to their propagation direction [17]. For the fourfold degenerate $(\pm 1, 0)$ and $(0, \pm 1)$ SPP modes, only $(0, \pm 1)$ modes can be excited under TE-polarized incident light. k_{\parallel} has no projection along the directions $(0, \pm 1)$, so the modes remain degenerated and no splitting can be observed upon the change of incident angle. This is what we observed above and has been observed by other groups [4]. However, for Si(1,1) modes which propagate in the direction $(\pm 1, \pm 1)$ k_{\parallel} and E_{\parallel} have a 45° or 135° angle with respect to the propagation direction of SPPs, respec-

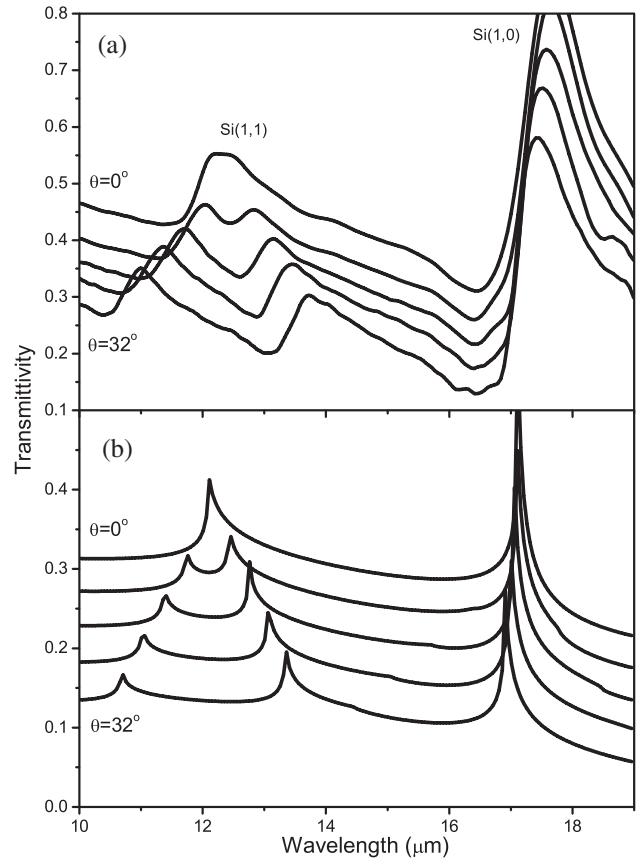


FIG. 2. (a) Experimental and (b) theoretical results of transmittivity of sample D under TE-polarized illumination. Shown in the figure are representative spectra at incident angles from 0° to 32° with a step of 8° . Consecutive curves have been shifted a value of 0.04 upwards to improve readability.

tively. All four modes can be excited and k_{\parallel} has a component along their propagation directions. According to Eq. (1), k_{\parallel} will be added to or subtracted from the reciprocal vectors, depending on the propagation direction. So the degeneracy of the $(\pm 1, \pm 1)$ modes will be lifted off, and the Si(1, 1) peak shows a splitting. The dispersion curves for both polarizations are displayed in Fig. 3. The theoretical ones extracted from Fig. 2(b) and calculated based on SPPs model are also presented. The experimental curves for TE and TM polarization are similar and fit fairly well with the theoretical ones. It is noticed that the two peaks under TM polarization are broader and weaker than their counterparts under TE polarization. This is because TM light penetrates deeper into the metal and gets absorbed more strongly than TE light.

The similar splitting characters of Si(1, 1) under TE and TM polarizations clearly confirm the involvement of SPPs during the transmission process. We note that Ref. [8] has successfully predicted the experimental results through Huygens diffraction model. According to Refs. [8,18], we believe that strong interplane coupling would hinder the observation of the splitting behavior under TE polarization. The strong coupling could be the reason that in previous work no splitting in the TE polarization has been reported.

The discussion above also applies well to the high order peaks of Si(2, 0), (2, 1), and (2, 2). Under TE polarization, Si(2, 0) makes minor blueshift (from $8.66 \mu\text{m}$ at 0° to $8.47 \mu\text{m}$ at 36°), which is similar to Si(1, 0). Si(2, 1) stays nearly unchanged since it will split into 4 branches, making the splitting hard to detect. Si(2, 2) is at $6.35 \mu\text{m}$ at 0° , then splits into two branches, which are at 5.95 and $6.63 \mu\text{m}$ at 16° . This behavior is similar to Si(1, 1). The change for high order peaks is generally not as significant

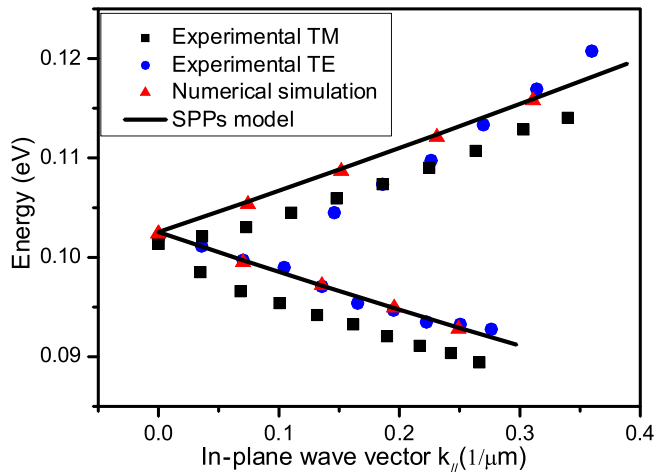


FIG. 3 (color online). Dispersion relation of Si(1,1) of sample D. For TE and TM polarizations, the incident angle in the experiment changes from 0° to 36° with a step of 4° . The numerical calculation result is extracted from Fig. 2(b). The solid line is the theoretical curve calculated by SPP model.

as the lower order ones. The reason is that the reciprocal vectors for high order peaks are large, making them less sensitive to the change of the in-plane vector of the incident light.

To verify that the interplane coupling is indeed very weak in the present system, we fabricated a series of Pt films with different thickness ranging from 220 to 50 nm and did the same measurements. All the peaks stay unchanged in wavelength until being overlapped by other peaks or merged into the background as the thickness decreases. Further numerical calculations on sample D with various thicknesses are made. The calculated transmission spectra of these samples under TE-polarized illumination at an incident angle of 16° are displayed in Fig. 4. The resonant peaks stay unchanged in wavelength while the thickness changes over 7 times from 120 to 920 nm, which clearly manifests the character of decoupled SPPs [19,20]. The splitting behavior does not change with the thickness, as long as the interplane coupling is weak. The situation is the same at other incident angles.

We notice that although most existing relevant theories treat the holes in the array as point scattering centers, it is expected that the finite size of the hole diameter will modify the exact behavior of the diffraction [21–24]. It is found that when the diameter of the holes is larger than half of the periodicity, the (1, 0) peak will split into two [25]. The reduced interference between the SPPs at two interfaces in the current system facilitates the study of the influence of hole diameter on the SPP assisted diffraction process. To this end, we fabricated sample E with thickness of 320 nm, lattice constant of $6 \mu\text{m}$, and hole diameter of $4 \mu\text{m}$, and compare the zeroth-order normal-incidence transmission of samples B and E, which are only different in hole diameters, as shown in Fig. 5. The most distinguished difference between the two spectra is around

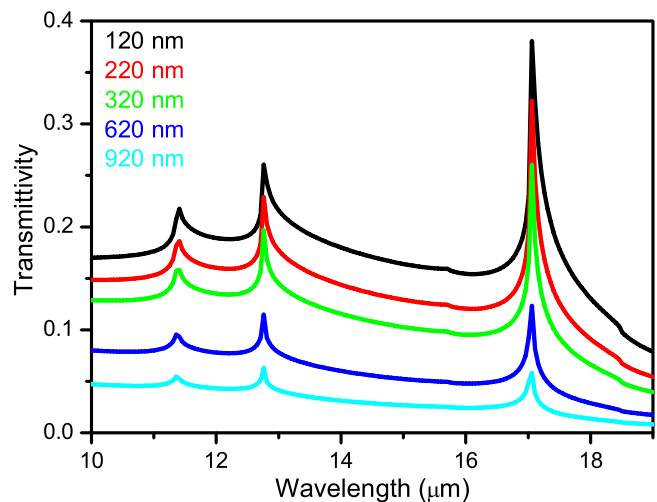


FIG. 4 (color online). Theoretical transmittivity of sample D with various film thickness. The illumination is TE polarized, with an incident angle of 16° .

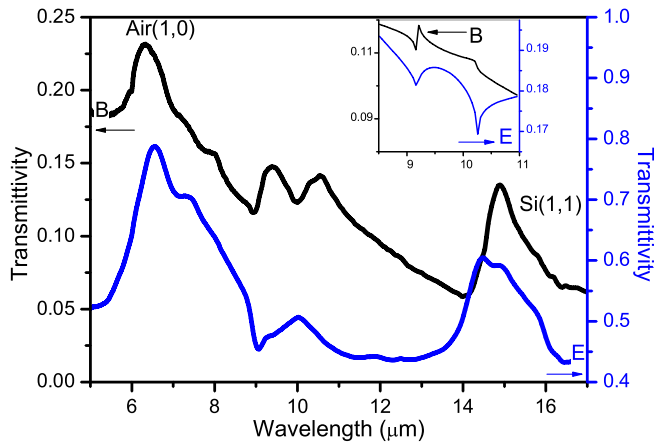


FIG. 5 (color online). Experimental and theoretical (inset) results of transmittivity of sample B (diam = 3 μm) and E (diam = 4 μm) under normal illumination.

10 μm where Si(2, 0) and (2, 1) in sample B seem to get merged in sample E. The theoretical result confirms such a phenomenon, as can be found in the inset of Fig. 5.

Since SPPs on the opposite interfaces overlap more for larger holes, one may attribute this phenomenon to the enhancement of the interplane coupling. We believe it is not the real reason. First, the wave vectors of SPPs corresponding to Si(2, 0) and (2, 1) are quite different from those of air(1, 0). There could not be any strong coupling. Second, we have done the angular dependence experiments of sample D and obtain similar results. As discussed previously, this verifies that interplane coupling is weak in these samples.

We attribute this change to the in-plane Bragg scattering of SPPs. When the hole diameter exceeds half of the periodicity, Bragg scattering will introduce band gaps to the dispersion relation, which correspond to different distributions of charges and electromagnetic field in space [26]. SPPs corresponding to the high order peaks have small wavelengths, so they are more sensitive to the actual size of the holes. We also find through numerical calculation that high order peaks are usually sharper and more pronounced when the hole diameter is smaller.

In summary, by adopting Si which has a large dielectric constant in comparison to air in the midinfrared regime and metal films of large thicknesses, we succeed in investigating the properties of SPPs at individual interfaces. The enhanced transmission is observed in an extended wavelength regime and transmission peaks with highest order up to (2, 2) are clearly revealed and fit well with the in-plane propagation characters of SPPs. The splitting of peaks Si(1, 1) is observed in TE and TM polarization, which confirms that the enhanced transmission is a SPP assisted diffraction phenomenon. Numerical calculations on the transmission spectra have been made and the results agree excellently with the experimental data. The agreement

between the numerical calculations and experimental results, together with the successful explanation of the experimental results based on SPPs, further clearly confirms the role played by SPPs in the enhanced transmission. Since Si is the base material for modern microelectronic applications, the extended working wavelength regime for the subwavelength optics makes the current system of this study a potential prototype element in future plasmonic circuits which can merge photonics and electronics at nanoscale dimensions.

The authors thank M. P. van Exter, C. Genet, W. M. Liu, and J. J. Hu for enlightening advice, and C. Z. Bi, Q. Luo, and H. F. Yang for technical help. This work is supported by National Science Foundation of China (No. 10674168 and No. 10525419), the MOST of China (973 project No. 2006CB601006), and project ITSNEM of the Chinese Academy of Sciences.

*xgqiu@aphy.iphy.ac.cn

- [1] T. W. Ebbesen *et al.*, Nature (London) **391**, 667 (1998).
- [2] G. Gay *et al.*, Phys. Rev. Lett. **96**, 213901 (2006).
- [3] M. M. J. Treacy, Phys. Rev. B **66**, 195105 (2002).
- [4] W. L. Barnes *et al.*, Phys. Rev. Lett. **92**, 107401 (2004).
- [5] F. Przybilla *et al.*, J. Opt. A Pure Appl. Opt. **8**, 458 (2006).
- [6] L. Martín-Moreno *et al.*, Phys. Rev. Lett. **86**, 1114 (2001).
- [7] A. Krishnan *et al.*, Opt. Commun. **200**, 1 (2001).
- [8] C. Genet, M. P. van Exter, and J. P. Woerdman, J. Opt. Soc. Am. A **22**, 998 (2005).
- [9] D. Sarid, Phys. Rev. Lett. **47**, 1927 (1981).
- [10] J. A. Dionne *et al.*, Phys. Rev. B **72**, 075405 (2005).
- [11] F. Miyamaru and M. Hangyo, Appl. Phys. Lett. **84**, 2742 (2004).
- [12] H. Y. Sang, Z. Y. Li, and B. Y. Gu, J. Appl. Phys. **97**, 033102 (2005).
- [13] H. Raether, *Surface Plasmons on Smooth and Rough Surfaces and on Gratings* (Springer-Verlag, Berlin, 1988).
- [14] H. F. Ghaemi *et al.*, Phys. Rev. B **58**, 6779 (1998).
- [15] M. A. Ordal *et al.*, Appl. Opt. **22**, 1099 (1983).
- [16] E. D. Palik, *Handbook of Optical Constants of Solids* (Academic, London, 1985).
- [17] L. Salomon *et al.*, Phys. Rev. Lett. **86**, 1110 (2001).
- [18] D. Gérard *et al.*, Opt. Express **12**, 3652 (2004).
- [19] A. Degiron *et al.*, Appl. Phys. Lett. **81**, 4327 (2002).
- [20] J. A. Porto, F. J. García-Vidal, and J. B. Pendry, Phys. Rev. Lett. **83**, 2845 (1999).
- [21] J. B. Pendry, L. Martín-Moreno, and F. J. Garcia-Vidal, Science **305**, 847 (2004).
- [22] S. Fasel *et al.*, Phys. Rev. Lett. **94**, 110501 (2005).
- [23] K. J. K. Koerkamp *et al.*, Phys. Rev. Lett. **92**, 183901 (2004).
- [24] F. J. García-Vidal *et al.*, Phys. Rev. Lett. **95**, 103901 (2005).
- [25] M. W. Tsai *et al.*, Appl. Phys. Lett. **88**, 213112 (2006).
- [26] S. A. Darmanyan and A. V. Zayats, Phys. Rev. B **67**, 035424 (2003).